19th Australasian Fluid Mechanics Conference
Melbourne, Australia
8-11 December 2014

Dynamics of a Quasi-Two-Dimensional Wake Behind a Cylinder in an MHD Duct Flow with a Strong Axial Magnetic Field

A. H. A. Hamid[1,2], W. K. Hussam[1] and G. J. Sheard[1]

[1]The Sheard Lab, Department of Mechanical and Aerospace Engineering, Monash University, Victoria 3800, Australia

[2]Faculty of Mechanical Engineering, Universiti Teknologi MARA, 40450 Selangor, Malaysia

Abstract

A confined laminar viscous flow past a two-dimensional bluff body in the presence of a strong uniform magnetic field is considered. The effects of Reynolds number (*Re*) and Hartmann number (*Ha*) on the dynamics of the wake are examined, with a focus on the shedding frequency and the distribution of the wake vortices. These two parameters are of primary interest as they play an important role in determining the mixing and heat transfer properties of the downstream flow. The results indicates that the imposed magnetic field significantly alters the dynamic behaviour of the wake behind a cylinder.

Introduction

It is well-known that beyond a critical *Re*, the flow around a circular cylinder generates a regular pattern of vortices known as the Kármán vortex street [9]. Analysis of such bluff body wakes are typically divided into three main focus areas: the correlation between drag coefficient, base pressure and shedding frequency; the vortex dynamics, where the formation and re-arrangement process are addressed; and the stability of the mean velocity profile in the wake [10].

For low Reynolds number ($50 < Re < 150$), the vortices are shed in a half-wavelength staggered array. Classically the vortex street within this Reynolds number range has been divided into three distinct regions, namely the formation region, the stable region, and the unstable region [12]. The formation region occurs immediately behind the cylinder, where the vorticity dissipates and organises into a coherent structure [9]. It has been shown in previous studies that the formation process plays a significant role in determining the shedding frequency and other wake behaviours [9, 12]. In general, the increase of turbulence level leads to higher shedding frequency. Succeeding the formation region is the stable region, where [12] found that the wake advection velocity is about 90% of the free stream velocity. As the vortices advected further downstream, the viscous effect has become less dominant and eventually leads to vortex street breakdown. A new, larger vortical structure evolves indicating the beginning of the unstable region. This secondary street possess a longer wavelength than the primary street and contains more than one dominant frequency [1].

When a strong magnetic fluid is imposed to a conducting fluid, the resulting wake possesses a distinct features as compared to the normal hydrodynamic flows. Typical example of such flows is in fusion power-reactor breeding blankets, where an electrically conducting fluid flows in channels within the blankets under a strong plasma-confining magnetic field. This class of flows are known as magnetohydrodynamic (MHD). The interaction between induced electric currents and the applied magnetic field results in an electromagnetic Lorentz force, which in turn gives a damping effect to the flow [14, 5] and subsequently alters the formation of vortex street.

It has been shown in previous studies that the wake stability is influenced by the near-wake behaviour [7] and the vortex trajectories [9]. While a great deal of attention has been paid to wake vortices in hydrodynamic (HD) flow, less attention has been paid to magnetohydrodynamic (MHD) counterparts. This is despite the potential application of bluff-body turbulence promoters for enhancement of heat transport in ducts within magnetic-confinement fusion reactor blankets [6]. An example of such work in MHD flows is by [3], where they did parametric study of the cylinder wake evolution at high *Re* and *Ha* regime. They found that for a given *Re*, wake formation length and shedding frequency increases as *Ha* is decreased. In the current work, particular attention is given to the low *Re* regime, motivated by the typical low velocity operating condition in fusion reactor application [16]. Furthermore, the low *Re* regime means that the wake behaviour under the effect of magnetic field can be directly compared with the hydrodynamic counterpart cases. To the best of the authors' knowledge, no such comparison has been made. The findings of the current work will furnish valuable information for promoting heat transfer in fusion-related duct flows.

Numerical Method and Validation

In the current investigation a flow of electrically conducting fluid passing over a circular cylinder placed on the centreline of a duct is considered. Figure 1 depicts the numerical domain and the corresponding macro-element mesh. The ratio of cylinder diameter to the duct width (i.e. blockage ratio, $\beta = d/2L$) is fixed at 0.1 throughout this study. Also shown in the figure is a typical Hartmann velocity profile, characterized by a flat profile in the core with velocity U_0 and high gradients in the vicinity of the lateral walls. The length scale is normalized by the half channel width, *L*. However, for the sake of discussions, the *Re* and the geometrical length in the succeeding discussions are presented in cylinder diameter scale, *d*. The use of two different length scales in an MHD cylinder wake flows is inevitable: the two-dimensional linear braking term is govern by *Ha* and *L*, whereas the *Re* and thus the structure of the cylinder wake is govern by *d* [4]. A quasi-two-dimensional (Q2D) model for MHD duct flow [14] is employed. At present, generally the SM82 model is applicable for MHD duct flows under the influence of strong magnetic field, although some deviation from the quasi-2D behavior can be observed in some situations, e.g. in complex geometry ducts. In the case of simple rectangular duct flows, SM82 has been verified against 3D results. The error using this model with the three-dimensional solution has been shown to be in order of 10% [3]. Under this model, the non-dimensional magnetohydrodynamic equations of continuity and momentum reduce to

$$\nabla \cdot \mathbf{u} = 0, \tag{1}$$

$$\frac{\partial \mathbf{u}}{\partial t} = -(\mathbf{u}\cdot\nabla)\mathbf{u} - \nabla p + \frac{1}{Re}\nabla^2\mathbf{u} - 2\frac{Ha}{Re}\mathbf{u}, \tag{2}$$

where $\mathbf{u}$ and p are the velocity and pressure fields, respectively. The governing equations are discretized using a high-order, in-house solver based on the spectral-element method.

To validate the numerical scheme being used, dimensionless

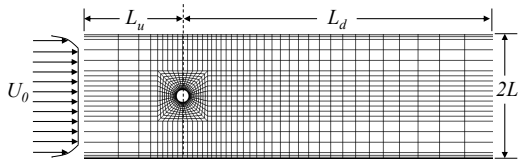

Figure 1. Schematic diagram of numerical domain and macro-element distribution.

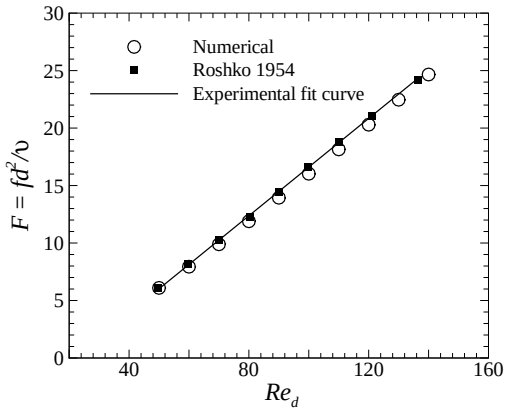

Figure 2. $F - Re$ plot of experimental data by [11] and current numerical results.

shedding frequency data from [11] is compared with the results obtained from the current simulations and the simulated results match well with the experimental data (refer figure 2). Further validation of the code can be found in [6, 5].

A grid independence study for spatial resolution has been performed by varying the element polynomial degree across a wide range, while keeping the macro element distribution unchanged. The mesh near the lateral walls and the cylinder was refined to resolve the anticipated high gradients, especially with the flows involving strong magnetic fields (refer figure 1). The monitored parameters (i.e. the pressure and viscous component of the time-averaged drag coefficient, $C_{D,p}$ and $C_{D,\mathrm{visc}}$ respectively, and the shedding frequency, St) revealed good convergence when the polynomial order increases. Polynomial degree 7 produced at most a 0.1% error, and is therefore used hereafter.

Result and Discussion

In all simulations, two basic regions of wake vortices are apparent; a formation region in which the vorticity evolved from cylinder boundary-layers organises into a vortex street, and a stable region in which the shed vortices convect downstream in a periodic laminar manner. This section presents the results of shedding frequency analysis and vortex distributions.

Shedding Frequency Analysis

In the current investigation, the effect of axial magnetic field on shedding frequency is of interest. The dependencies of Ha and Re on the shedding frequency are illustrated in figure 3. It is to be noted that $H = 0$ correspond to hydrodynamic flows. The dimensionless frequency is represented by the Strouhal number, $St = fd/U_0$, where f is shedding frequency, calculated from the fluctuating lift force imparted on the cylinder due to the near-wake flow unsteadiness.

As figure 3 indicates, the Strouhal number is dependent on both

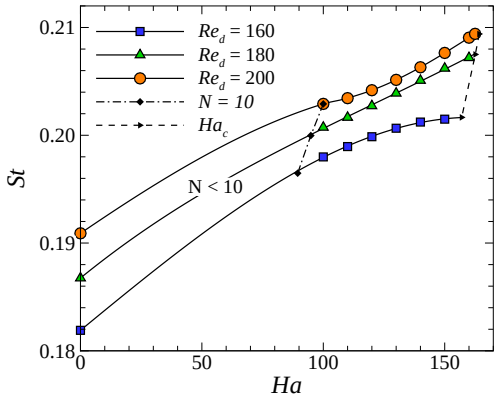

Figure 3. Variation of the Strouhal number. The symbols connected by the dashed-dotted line indicate $N = 2\beta Ha^2/Re = 10$ for each correponding Re_d. Ha lower than these values results in $N < 10$, which violates the validity of the Q2D model currently employed. The symbols connected by the dashed line indicate the critical Ha, beyond which results in a complete suppression of vortex shedding due to Hartmann braking [6].

Ha and Re. In the range of the Ha and Re considered in this study, St increases with increasing Ha at a given Re. This observation can be attributed to the fact that the imposed magnetic field tends to stretch the shear layer at the near wake, and hence mass conservation requires that the wake advection velocity, U_ω is increased. It can be seen in figure 4 that stronger magnetic field intensity produces a narrower wake, thus extending the formation region behind the cylinder before the shear layer roll up into a vortex street.

The accelerating effect of the magnetic field on the wake advection is illustrated in figure 5. The increase in U_ω as Ha is increased explains the increase in St. It is also interesting to note that at a given Ha, St increases but U_ω decreases with increasing Re. In this case, the increase in St cannot be associated with an increase of U_ω, but rather to the increased vorticity production rate as Re is increased. At high Re, the vorticity attached to the cylinder quickly organises into a coherent structure due to the high rate of vorticity supply, thus the duration associated with the formation of vortex shedding becomes shorter, leading to a shorter formation length and a higher St.

In order to verify this argument, the formation length, L_F, has been measured and the results are presented in table 1. The formation length is defined as a distance from the rear of the cylinder to the position of first shed vortex peak strength [9]. The measurement error, $\varepsilon_{L_F}/\lambda$ presented in table 1 is associated with the phase gap between two consecutive snapshots, i.e. 0.25π (which corresponds to nine snapshots per shedding cycle). The maximum error per wavelength is 11%, where the wavelength is calculated by employing the Taylor hypothesis (which is valid since the present case is in laminar flow regime), i.e. $\lambda = U_\omega/f$. It is found that the distance taken for the vorticity to complete its formation decreases as Re is increased, which supports the aforementioned statement. This trend is also in agreement with the experimental results of the HD counterpart [12, 15]. Furthermore, the decrease in the formation length is more prominent at higher Ha value.

This argument also explains the contradicting trend of St at higher Re regime as reported by [3]. They found that at a given Re, the St decreases with increasing Ha. At a higher Re, the rate of vorticity production is increased, thus reducing the ac-

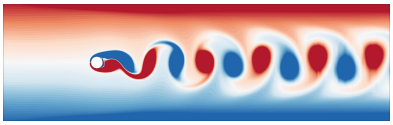

(a) $Ha = 0$

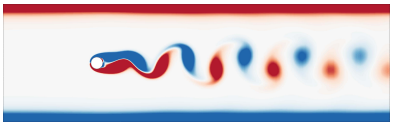

(b) $Ha = 100$

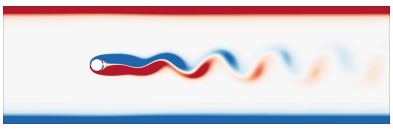

(c) $Ha = 150$

Figure 4. Contour plots of vorticity snapshot at $Re_d = 160$ and at Hartmann number as indicated. Contour levels ranges between -2 and 2, with red and blue countours representing negative and positive vorticity, respectively.

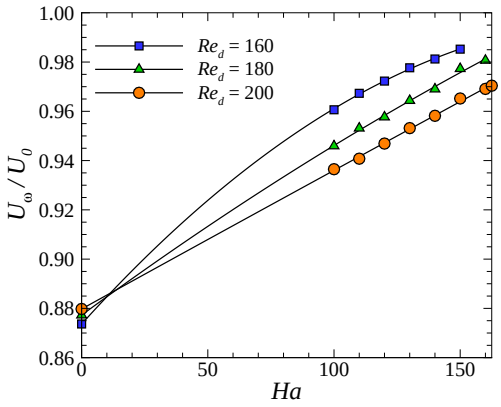

Figure 5. Advection velocity of wake vortices. The velocites are calculated at the stable region of the wake, where the vortices advected downstream at almost contant velocity. The line is a 2nd order polynomial fit of the data.

celeration effect due to the near wake contraction. At this point, as Ha increases, the opposing Lorentz force becomes dominant and hence the St is decreased. It is important to note that in the current simulations, the magnetic field was imposed in the axial direction. However, when the magnetic field is transverse to the cylinder, previous investigation [13] has found that St is not influenced by the change in Ha for a fixed Re.

Vortex Distributions

Vortex trajectories along the computed domain have been recorded based on the locations of peak vorticity. In all cases, the trajectories of positive and negative vorticity show a symmetric profile with respect to the wake axis. From these trajectories, lateral spacing (h) and longitudinal spacing (l) of the vortices has been computed and normalized by the cylinder diameter. The lateral spacing is defined as the vertical distance between peak vorticity of adjacent opposite-sign vortices, or twice the distance between a peak vorticity of either a positive or negative-signed vortex and the wake centerline (for a symmetric vortex shedding). The longitudinal spacing is defined as the distance between successive vortices of the same sign.

Ha	Re_d	L_F	ε_{L_F}	λ	$\varepsilon_{L_F}/\lambda$ (%)	l_{avg}
0	160	0.80	0.17	4.80	3.6	4.80
	180	0.78	0.14	4.70	3.0	4.69
	200	0.68	0.12	4.61	2.7	4.61
100	160	1.48	0.26	4.85	5.5	4.86
	180	1.18	0.18	4.71	3.9	4.72
	200	0.94	0.19	4.62	4.1	4.62
125	160	1.81	0.29	4.87	6.0	4.87
	180	1.45	0.22	4.72	4.6	4.73
	200	1.13	0.20	4.64	4.3	4.64
150	160	2.69	0.52	4.89	10.6	4.91
	180	1.67	0.35	4.74	7.4	4.74
	200	1.33	0.20	4.65	4.4	4.65

Table 1: Vortex shedding formation length and longitudinal length. The formation length is measured from the rear of the cylinder and both length are non-dimensionalized by the cylinder diamter.

The spatial evolution of lateral spacing is presented in figure 6. For brevity, only cases with $Ha = 0$ and cases with highest Ha, i.e. $Ha = 150$ are shown. A very distinctive wake pattern was observed between the two classes of flows. When the magnetic field is absent, the lateral spacing first decreases to zero at a distance about 130-160% of its respective wavelength (shown by the dotted lines). At this position, an inversion of the wake takes place, where vortices cross the wake centreline to the side opposite to that on which they formed. After this the lateral spacing increases along the computed domain. By referring to figure 4(a), it is apparent that the inversion mechanism is the entrainment of vorticity from the free stream into the wake, which tends to push the vortex towards the inverted position. It is also important to note that the distance at which the wake inverts from the cylinder decreases when Re is increased, which is in agreement with the previous findings [2]. However, in the presence of a magnetic field, no wake inversion takes place, at least along the length of the computed domain. By inspecting the decay of wake vortices, it is expected that inversion will never takes place for MHD flow at this particular β. In contrast, wake inversion will eventually occur in $Ha = 0$s flow even for a low β [2]. This can be explained due to the fact that in the presence of magnetic field, the Lorentz force tends to flatten the incoming flow velocity profile, which eliminates vorticity from the core flow. As a result, the wake vortices advect downstream in an almost parallel manner (as indicated by the small gradient of the MHD data in figure 6) without interaction with the free stream vorticity. While there is no appreciable difference in h for all Re in HD flows, h decreases as Re is increased in MHD flows. As Re is increased, the rate of vorticity supply to the shear layer attached to the cylinder increases. As a result, the tip of the shear layer tends to rolls up further towards the wake axis, narrowing the wake. Furthermore, it can be seen that the wake is wider under the influence of a magnetic field than the corresponding non-MHD wake, regardless of the flow Re. This observed widening is supported by the previous 3D simulation by [8].

On the other hand, the longitudinal spacing is almost constant for a given Ha and Re, except in the formation region, where l increases until the vortex stabilizes. Here, the local value of l is not important, and therefore only its mean values are presented in table 1. It is important to note that the local l was determined from the phase diagram, and that the average value was calculated over the stable region. These average values are comparable with the wavelength calculated previously, which strengthens the previous argument that the wake flow is

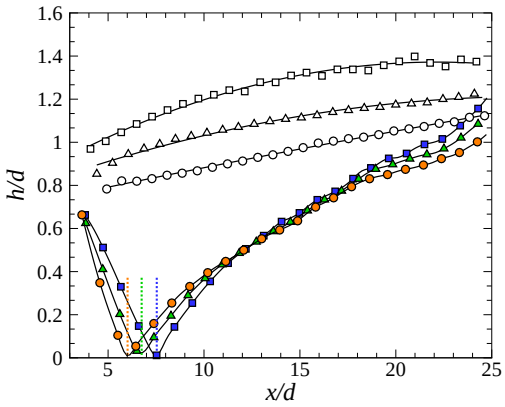

Figure 6. Spatial variation of vortex lateral spacing. Solid symbols show $Ha = 0$ and open symbols show $Ha = 150$. Square, delta and circle symbols represent $Re_d = 160, 180$ and 200, respectively.

laminar. Also to be noted is that l_{avg} increases as Ha is increased and Re is decreased, and that l_{avg} is more sensitive to changes in Re than Ha. To understand this, one need to realize that the non-dimensional shedding frequency is given by $St = (U_0 - V)/l = U_\omega/l$ [11]. Although both St and U_ω increase as Ha is increased, the increment of U_ω is more prominent compared to St , which explains the increase in l for increased Ha. A similar argument applies to the HD flows, where the reduction in St is more significant compared to U_ω when Re is decreased. The explanation of the increased l as Re is decreased in MHD flows is more straightforward: reduction in Re leads to lower St and higher U_ω.

Conclusion

The present study has investigated the characteristics of wakes behind a circular cylinders in a rectangular duct under a strong axial magnetic field using a spectral-element method. It is found that the formation of vortex shedding and the direction of the imposed magnetic field play significant roles in determining the shedding frequency. The present investigation reveals that an axial magnetic field tends to appreciably increase the St, regardless of flow Re. Furthermore, the advection speed of wake vortices is also a strong function of both Ha and Re, whereas U_ω is only weakly dependent on Re for hydrodynamic flows. An increase in Ha leads to higher U_ω. It follows then that the longitudinal spacing of wake vortices is also affected since the wake parameters are interdependent. In addition, the incoming flow vorticity plays important role in the lateral dispersion of wake vortices and thus the wake inversion phenomenon. In the absence of a magnetic field, the wake inverted at about 6 - 8 diameter downstream from the centre of the cylinder. However, in the presence of a magnetic field, two nearly parallel rows of vortices in a staggered arrangement resembling an ideal Kármán vortex street was observed.

Acknowledgements

This research was supported by ARC Discovery Grant DP120100153, high-performance computing time allocations from the National Computational Infrastructure (NCI) and the Victorian Life Sciences Computation Initiative (VLSCI), and the Monash SunGRID. A. H. A. H. is supported by the Malaysia Ministry of Education and the Universiti Teknologi MARA, Malaysia.

References

[1] Bühler, L., 1996, Instabilities in quasi-two-dimensional magnetohydrodynamic flows, *Journal of Fluid Mechanics*, **326**, 125–150.

[2] Camarri, S. and Giannetti, F., 2007, On the inversion of the von Kármán street in the wake of a confined square cylinder, *Journal of Fluid Mechanics*, **574**, 169–178.

[3] Dousset, V. and Pothérat, A., 2008, Numerical simulations of a cylinder wake under a strong axial magnetic field, *Physics of Fluids*, **20**, 017104.

[4] Frank, M., Barleon, L. and Müller, U., 2001, Visual analysis of two-dimensional magnetohydrodynamics, *Physics of Fluids*, **13**, 2287.

[5] Hussam, W. K. and Sheard, G. J., 2013, Heat transfer in a high hartmann number MHD duct flow with a circular cylinder placed near the heated side-wall, *International Journal of Heat and Mass Transfer*, **67**, 944–954.

[6] Hussam, W. K., Thompson, M. C. and Sheard, G. J., 2011, Dynamics and heat transfer in a quasi-two-dimensional MHD flow past a circular cylinder in a duct at high hartmann number, *International Journal of Heat and Mass Transfer*, **54**, 1091–1100.

[7] Hussam, W. K., Thompson, M. C. and Sheard, G. J., 2012, Optimal transient disturbances behind a circular cylinder in a quasi-two-dimensional magnetohydrodynamic duct flow, *Physics of Fluids (1994-present)*, **24**, 024105.

[8] Kanaris, N., Albets, X., Grigoriadis, D. and Kassinos, S., 2013, Three-dimensional numerical simulations of magnetohydrodynamic flow around a confined circular cylinder under low, moderate, and strong magnetic fields, *Physics of Fluids (1994-present)*, **25**, 074102.

[9] Kieft, R. N., Rindt, C., Van Steenhoven, A. and Van Heijst, G., 2003, On the wake structure behind a heated horizontal cylinder in cross-flow, *Journal of Fluid Mechanics*, **486**, 189–211.

[10] Monkewitz, P. and Nguyen, L., 1987, Absolute instability in the near-wake of two-dimensional bluff bodies, *Journal of Fluids and Structures*, **1**, 165–184.

[11] Roshko, A., 1954, On the development of turbulent wakes from vortex streets, *National Advisory Committee for Aeronautics*.

[12] Schaefer, J. W. and Eskinazi, S., 1959, An analysis of the vortex street generated in a viscous fluid, *Journal of Fluid Mechanics*, **6**, 241–260.

[13] Singha, S. and Sinhamahapatra, K., 2011, Control of vortex shedding from a circular cylinder using imposed transverse magnetic field, *International Journal of Numerical Methods for Heat & Fluid Flow*, **21**, 32–45.

[14] Sommeria, J. and Moreau, R., 1982, Why, how, and when, MHD turbulence becomes two-dimensional, *Journal of Fluid Mechanics*, **118**, 507–518.

[15] Szepessy, S. and Bearman, P., 1992, Aspect ratio and end plate effects on vortex shedding from a circular cylinder, *Journal of Fluid Mechanics*, **234**, 191–217.

[16] Tagawa, T., Authié, G. and Moreau, R., 2002, Buoyant flow in long vertical enclosures in the presence of a strong horizontal magnetic field. part 1. fully-established flow, *European Journal of Mechanics-B/Fluids*, **21**, 383–398.